

Fluorescence quenching in graphene: a fundamental ruler and evidence for transverse plasmons

G. Gómez-Santos and T. Stauber

*Departamento de Física de la Materia Condensada and Instituto Nicolás Cabrera,
Universidad Autónoma de Madrid, E-28049 Madrid, Spain*

Graphene's fluorescence quenching is studied as a function of distance. Transverse decay channels, full retardation and graphene-field coupling to all orders are included, extending previous instantaneous results. For neutral graphene, a virtually exact analytical expression for the fluorescence yield is derived, valid for arbitrary distances and only based on the fine structure constant α , the fluorescent wavelength λ , and distance z . Thus graphene's fluorescence quenching measurements provide a fundamental distance ruler. For doped graphene and at appropriate energies, the fluorescence yield at large distances is dominated by transverse plasmons, providing a platform for their detection.

PACS numbers: 78.67.Wj, 78.70.En, 73.20.Mf, 42.25.Bs

I. INTRODUCTION

The optical properties of graphene have attracted immense attention due to the potential applications in the field of photonics and optoelectronics¹. Absorption, for instance, has the universal value $\approx \pi\alpha$ for light in the visible spectrum, depending on the fine structure constant α , but not on material's properties^{2,3}, providing a decisive clue for its original identification⁴. The large intrinsic carrier mobilities and doping tunability have led to a number of proposals for optoelectronic applications^{1,5-7}, where the engineering of long-lived graphene's plasmons could play a major role⁸⁻¹⁰.

Graphene (and its oxide) exhibits excellent quenching of nearby fluorescent materials¹¹⁻¹⁴, a property shared with carbon nanotubes^{15,16}. This technique has allowed spectacular contrast images, enabling far easier optical identification¹² (and prospects for device manipulation¹⁷) of graphene's flakes. Given the mature nature of fluorescent microscopy, particularly in the biological sciences, their combination with increasingly available and versatile graphene nanostructures could open interesting research directions¹⁴. Furthermore, graphene's fluorescence quenching has also been proposed as a convenient probe of the intrinsic excitations of doped graphene such as plasmons¹⁸.

Here, we theoretically address the effect of graphene on the fluorescent material's yield as function of the distance z within a unifying formalism. By this, we discuss for the first time the transverse decay channels known to lead to characteristic features only found in graphene.¹⁹ The process implies non-radiative (Förster^{20,21}) decay of the excited dye, with energy transfer to graphene's excitations. This mechanism is expected to dominate over competing charge-transfer processes except, perhaps, in near contact situations^{22,23}. Our motivation stems from the seemingly paradoxical coexistence in graphene of very strong fluorescence quenching and nominally weak coupling to the electromagnetic field, as judged from the absorption results.

The distance behavior of fluorescence quenching as function of the distance z of a dye molecule with respect to a metal surface was found long ago to be z^{-4} .²⁴ This law has repeatedly been found in subsequent studies of energy transfer involving various kinds of nanomaterials.²⁵ For graphene, the topic has been discussed by Swathi and Sebastian, treating the (instantaneous) longitudinal coupling between graphene and fluorescent material to lowest order, and again obtaining the z^{-4} -law.²⁶ Here, we extend their calculations in three significant ways: i) we include transverse decay channels in the calculations ii) the coupling between graphene and the electromagnetic field is taken to all orders iii) we use the full (retarded) photon propagator.

Our results for undoped graphene are as follows: i) a compact, analytical approximation is obtained and shown to provide a virtually exact description of the fluorescent yield for all distances. This analytical expression only depends on the ratio of the distance to the emitting wavelength (z/λ) and the fine structure constant α . A fluorescence measurement thus becomes a distance ruler, based only on fundamental constants - a long sought goal of the field. ii) Retardation is shown to modify the z^{-4} law into a slower z^{-2} behavior, with the transverse decay channel dominating at long distances.

For doped graphene, we show that the fluorescence yield is mostly determined by the plasmonic modes¹⁸ where at certain frequencies transverse plasmons yield the dominant, extremely slowly decaying contribution at large distances. This should help to detect these modes characteristic to graphene and intimately linked to the chirality of its elementary excitations.

The paper is organized as follows. In section II, we introduce the formalism defining the atom-field coupling in the presence of graphene and the induced fluorescence quenching. In section III, we present our results and then close with a summary. In an appendix, details on the explicit form of the decay rates are given.

II. FORMALISM

A. Atom-field coupling in the presence of graphene

We consider a fluorescent atom modeled by a two level system and the electromagnetic field described in a gauge without scalar potential. Within the standard dipole approximation, an excited atom will decay into the ground state at a rate (γ) given by²⁷

$$\hbar\gamma = -2\omega^2 p_\alpha^* \text{Im}\mathcal{D}^{\alpha\beta}(\mathbf{r}, \mathbf{r}; \omega) p_\beta, \quad (1)$$

where \mathbf{p} is the dipole matrix element between ground and excited states, separated in energy by $\hbar\omega$. \mathcal{D} represents the retarded photon Green's function defined as usual,

$$\mathcal{D}^{\alpha\beta}(\mathbf{r}, \mathbf{r}'; \omega) = -\frac{i}{\hbar} \int_0^\infty dt e^{i\omega t} \langle [A_\alpha(\mathbf{r}, t), A_\beta(\mathbf{r}', 0)] \rangle, \quad (2)$$

where $\mathbf{A}(\mathbf{r})$ is the vector potential operator at the atom's location. Notice that Eq. (2) corresponds to the photon propagator without the fluorescent atom, but in the presence of graphene.

In vacuum (that is, *without* graphene), the photon Green's function $\mathcal{D}_0^{\alpha\beta}(\mathbf{r} - \mathbf{r}'; \omega)$ is given by the Fourier transform of $\mathcal{D}_0^{\alpha\beta}(\mathbf{k}, \omega) = \frac{\mu_0 c^2}{\omega^2 - c^2 k^2} (\delta_{\alpha\beta} - \frac{k_\alpha k_\beta}{k^2}) + \frac{1}{2\epsilon_0 \omega^2} \frac{k_\alpha k_\beta}{k^2}$. Later inclusion of graphene, assumed perpendicular to the z axis, will preserve the parallel (to graphene's plane) component of momentum, $\mathbf{q} = (q_1, q_2)$, as a good quantum number. Therefore, it is convenient to employ the following representation for the vacuum Green's function

$$\mathcal{D}_0^{\alpha\beta}(z, z'; \mathbf{q}, \omega) = \frac{1}{2\pi} \int dk_z e^{ik_z(z-z')} \mathcal{D}_0^{\alpha\beta}(\mathbf{k}, \omega), \quad (3)$$

with $\mathbf{k} = (\mathbf{q}, k_z)$. Physically, Eq. (3) represents the vector potential in a plane perpendicular to the z -axis located at the position z due to currents in a parallel plane at location z' .

The in-plane components of the tensor \mathcal{D}_0^{ij} , decomposed into longitudinal and transverse contributions, are given by

$$\mathcal{D}_0^{ij}(z, z') = d_l e^{-q'|z-z'|} \frac{q_i q_j}{q^2} + d_t e^{-q'|z-z'|} (\delta_{ij} - \frac{q_i q_j}{q^2}), \quad (4)$$

with $i(j) = 1, 2$ and $q' = \sqrt{q^2 - (\omega/c)^2}$. The functions $d_{l,t}(\mathbf{q}, \omega)$ are given by (dependencies removed for clarity)

$$d_l = \frac{q'}{2\epsilon_0 \omega^2}, \quad d_t = -\frac{c^{-2}}{2\epsilon_0 q'}. \quad (5)$$

The remaining tensor components are written as

$$\mathcal{D}_0^{iz}(z, z') = \mathcal{D}_0^{zi}(z, z') = \frac{iq_i}{q'} d_l e^{-q'|z-z'|} \text{sgn}(z - z') \quad (6)$$

and

$$\mathcal{D}_0^{zz}(z, z') = \frac{1}{\epsilon_0 \omega^2} \delta(z - z') - \frac{q^2}{q'^2} d_l e^{-q'|z-z'|}. \quad (7)$$

The presence of a graphene plane at the location z_1 modifies the vacuum Green's function as follows

$$\mathcal{D}^{\alpha\beta}(z, z') = \mathcal{D}_0^{\alpha\beta}(z, z') + \mathcal{D}_0^{\alpha i}(z, z_1) e^2 \chi^{ij} \mathcal{D}_0^{j\beta}(z_1, z'), \quad (8)$$

where sum over repeated indexes is assumed. e is the electron charge and $\chi^{ij}(\mathbf{q}, \omega)$ represents graphene's current-current total response to external fields. The latter, decomposed into longitudinal and transverse contributions, is given by

$$\chi^{ij} = \frac{\chi_l}{1 - e^2 d_l \chi_l} \frac{q_i q_j}{q^2} + \frac{\chi_t}{1 - e^2 d_t \chi_t} (\delta_{ij} - \frac{q_i q_j}{q^2}), \quad (9)$$

where we take the non-interacting (RPA), well-known expression for the longitudinal²⁸ and transverse²⁹ components at zero doping:

$$\chi_l = -\frac{g_s g_v}{16\hbar v} \frac{\omega^2}{\sqrt{q^2 - (\omega/v)^2}}, \quad \chi_t = \frac{g_s g_v}{16\hbar} v \sqrt{q^2 - (\omega/v)^2}, \quad (10)$$

with spin and valley degeneracies, $g_s = g_v = 2$, and graphene's velocity v . For finite doping, we refer to the expressions given in Refs.^{29,30}

The previous calculation of Swathi and Sebastian²⁶ would correspond to zero doping and retaining only the (numerator of the) longitudinal response (χ_l) in Eq. (9), while setting $c \rightarrow \infty$ in the photon propagator (instantaneous limit).

B. Fluorescence quenching

Consider the graphene sheet placed at the origin ($z_1 = 0$) and the excited atom at a distance z . The expression (1) for the decay rate can be decomposed as

$$\hbar\gamma_{nr} = -2\omega^2 p_\alpha^* \left\{ \frac{1}{(2\pi)^2} \int_{q \geq \omega/c} d^2 q \text{Im}\mathcal{D}^{\alpha\beta}(z, z) \right\} p_\beta, \quad (11)$$

with the (graphene's modified) photon Green's function given by Eq. (8). The \mathbf{q} label classifies the final field states into *evanescent* excitations ($q > \omega/c$), and *propagating* excitations ($q < \omega/c$), the latter being the observed photons. Therefore, the total decay rate is given by the radiative and non-radiative contributions to the decay rate,

$$\gamma = \gamma_{nr} + \gamma_r. \quad (12)$$

Let us consider the rate of *observed* photons Φ . In addition to $\gamma_{r,nr}$, it will depend on the rate at which the atom is pumped into the excited state γ_{exc} . Furthermore, not all propagating photons are observed, a fraction being later absorbed by graphene γ_{abs} . The excitation rate is hardly affected by the presence of graphene and the fraction of emitted photons later absorbed is, up to logarithmic corrections, of the order of the fine structure

constant ($\alpha = \frac{e^2}{4\pi\epsilon_0\hbar c}$). Therefore, the ratio of the total observed fluorescence when the atom is at distance z , $\Phi(z)$, to that at infinite distance, Φ_∞ , can be written as

$$\frac{\Phi(z)}{\Phi_\infty} = \left(1 + \frac{\gamma_{nr}}{\gamma_r}\right)^{-1}, \quad (13)$$

where the neglected terms amount to minute relative corrections of order α^2 in the expression (13).

III. RESULTS

A. Zero doping

We have evaluated the distance dependence to undoped graphene of the observed fluorescence, Eq. (13), with $\gamma_{r,nr}$ obtained from Eq. (11) and Eq. (8). There is a sharp difference in graphene's effect on the non-radiative and radiative contributions to the decay. Graphene modification of the (radiative) vacuum decay is a weak effect, proportional to α (up to logarithmic corrections). Therefore, setting $\gamma_r \approx \gamma_0$, with the vacuum decay rate given by $\hbar\gamma_0 = \frac{p^2\omega^3}{3\pi\epsilon_0c^3}$, the results can be written as

$$\frac{\gamma_{nr}}{\gamma_r} \approx \frac{\gamma_{nr}}{\gamma_0} = \beta_1\tilde{\gamma}_1\tilde{f}_1 + \beta_2\tilde{\gamma}_2\tilde{f}_2 + \beta_3\tilde{\gamma}_3\tilde{f}_3, \quad (14)$$

with the physically relevant magnitudes given by

$$\tilde{\gamma}_1 = \frac{3^2}{2^9\pi^3} \alpha \left(\frac{\lambda}{z}\right)^4 \quad (15a)$$

$$\tilde{\gamma}_2 = \frac{3}{2^6\pi} \alpha \left(\frac{\lambda}{z}\right)^2 \quad (15b)$$

$$\tilde{\gamma}_3 = \frac{3}{4} \pi \alpha g(2\pi^2\alpha z/\lambda) \xrightarrow{\frac{z}{\lambda} \gtrsim \frac{1}{2\pi^2\alpha}} \frac{3}{2^4\pi^3\alpha} \left(\frac{\lambda}{z}\right)^2, \quad (15c)$$

where the function $g(a)$ can be written in terms of the sine and cosine-integrals (si, ci) as

$$g(a) = -\text{ci}(a) \cos(a) - \text{si}(a) \sin(a). \quad (16)$$

The coefficients $\beta_{1,2,3}$ are mere geometric factors depending on the emitting dipole orientation, with $\beta_1 = (p_{||}^2/2 + p_z^2)/p^2$, $\beta_2 = p_z^2/p^2$, and $\beta_3 = (p_{||}^2/2)/p^2$. All information about graphene in Eq. (14) is relegated to the dimensionless factors \tilde{f}_i , derived and discussed in the appendix.

The first term, $\tilde{\gamma}_1$, coincides with the unretarded contribution to the decay into graphene's longitudinal (charged excitations), previously considered²⁶. The other two terms (15b) and (15c), absent in a non-retarded calculation, prevail at large distances. The contribution of Eq. (15b) comes from charged excitations whereas (15c) is due to transverse excitations. Quantitatively, it is the last term (15c), which provides the dominant large distance asymptotic behavior.

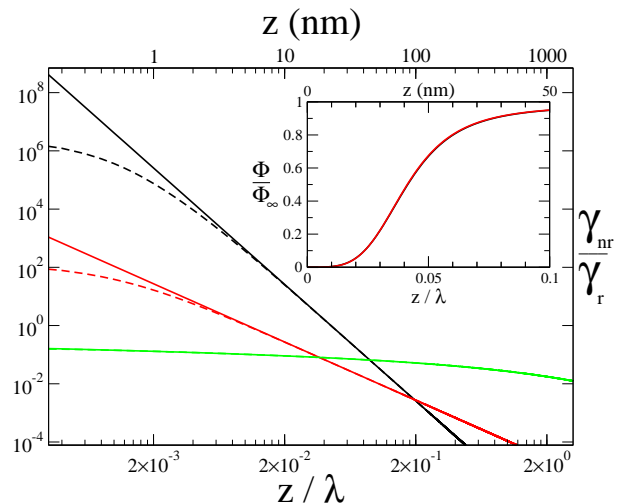


FIG. 1. Distance dependence of the analytical approximation for the decay channels ($\tilde{\gamma}_i$, solid lines) compared to the exact results ($\tilde{\gamma}_i\tilde{f}_i$, dashed lines). Black solid (dashed) line: $\tilde{\gamma}_1$ ($\tilde{\gamma}_1\tilde{f}_1$). Red solid (dashed) line: $\tilde{\gamma}_2$ ($\tilde{\gamma}_2\tilde{f}_2$). Green solid (dashed) line: $\tilde{\gamma}_3$ ($\tilde{\gamma}_3\tilde{f}_3$). (Exact results correspond to $\lambda = 500\text{nm}$). Inset: Fluorescence as a function of distance. Black line: exact result. Red line: analytical approximation.

B. Analytical approximation

Our analytical approximation consists in setting the functions \tilde{f}_i equal to one. The approximation $\tilde{f}_i \approx 1$ for $i = 1, 2$ holds when $x_0 \ll 1$ and $x_0^2(\frac{\pi^2\alpha_g^2}{4} - 1) \ll 1$, where $x_0 = \frac{1}{4\pi} \frac{v}{c} \frac{\lambda}{z}$, with *graphene's fine structure constant* $\alpha_g = \frac{c}{v}\alpha$. For graphene parameters, the latter condition dominates and can be recast as $x_0 \lesssim \frac{2}{\pi\alpha_g}$ or, equivalently, $\frac{z}{\lambda} \gtrsim \frac{\alpha}{8} \approx 10^{-3}$, justifying our analytical approximation. The approximation $\tilde{f}_3 \approx 1$ applies for $x_0 \ll 1$, implying $\frac{z}{\lambda} \gtrsim \frac{v}{4\pi c} \approx 10^{-4}$.

The exact and approximate non-radiative decays are plotted in Fig. 1. One sees that the approximation only fails in the extreme sub-wavelength regime. Furthermore, even though the exact decay rate saturates for $(z/\lambda) \rightarrow 0$ whereas the approximate one diverges, this saturation value is so huge that the difference between exact and approximate results has virtually no impact on Φ as seen in the inset of Fig. 1, where the exact and approximate curves are indistinguishable. Fig. 1 confirms that retardation channels, $\gamma_{2,3}$, control the decay at large distances, leading to a z^{-2} behavior dominated by graphene's transverse excitations of Eq. (15c).

C. Fundamental ruler

Notice that only α , z and λ appear in expressions (15), without any reference to graphene's properties. This implies that a measurement of the fluorescence quenching amounts to a measurement of the distance z , in terms of

the light's wavelength λ , and the fine structure constant α . In other words, it provides us with a *fundamental distance ruler*.

In general, one would expect graphene's properties to drop out from dimensionless optical properties involving graphene's excitation within the light-cone, such as the absorption. There, $\omega \gg vq$, and graphene's response becomes local, leaving α as the sole coupling scale. But a cursory application of this reasoning to our case would justify expressions like Eqs. (15) only for distances $z \gtrsim \lambda$, where graphene's light-cone excitations dominate. Surprisingly, the analytical expressions apply for virtually arbitrary short distances, implying graphene's excitations deep into the evanescent region where the q -dependence does not seem obviously negligible. A further surprise is the enormous efficacy of graphene as a fluorescence quencher, particularly in view of the nominally weak coupling with the field, set by α . Both facts, *range and strength*, can be explained if the naive nominal range for the expected disappearance of graphene's Fermi velocity v in the expressions $z \gtrsim \lambda$, can be extended to much shorter distances $z \ll \lambda$. Our approximations show that this is indeed the case. The blow up of $(\lambda/z)^4$ in the first term of Eq. (14) when $(z/\lambda) \rightarrow 0$, more than compensates the overall factor α , leading to strong quenching, as experimentally observed^{11–13}.

D. Finite doping

Graphene's fluorescence quenching in doped graphene due to graphene's longitudinal coupling to the light field has first been analyzed in Ref.¹⁸ within the unretarded approximation. For large frequencies, $\hbar\omega \gtrsim 2E_F$, the fluorescence yield of undoped graphene is obtained. For frequencies $\hbar\omega \lesssim 2E_F$, the quenching behavior is dominated by longitudinal plasmon excitations, leading to a characteristic exponential decay with distance.

Here, we extend the discussion by also analyzing the *transverse plasmon* excitations.¹⁹ These exist in the range $1.667 < \Omega \lesssim 2$ with $\Omega = \omega/(vk_F)$, leading to a decay rate, γ_t , which dominates at long-distances:

$$\hbar\gamma_t = \frac{\omega^2}{c^2} p_{||}^2 \frac{q'_p}{4\epsilon_0} e^{-2q'_p z} \frac{1}{1 - q'_p \frac{d}{dq'} \ln \chi_t|_{q'=q'_p}}, \quad (17)$$

where $q'_p = \sqrt{q_p^2 - (\omega/c)^2}$, with plasmon momentum q_p . Approximating graphene's transverse response by the long-wavelength limit, we obtain the following analytical expression:

$$\frac{\gamma_t}{\gamma_0} = \frac{3\pi}{2} \frac{p_{||}^2}{p^2} \frac{\alpha}{\Omega} f(\Omega) e^{-z/z_0} \quad (18)$$

with $z_0^{-1} = 4\alpha(v_F/c)k_F f(\Omega)$ and

$$f(\Omega) = \frac{\Omega}{4} \ln \left| \frac{2 + \Omega}{2 - \Omega} \right| - 1. \quad (19)$$

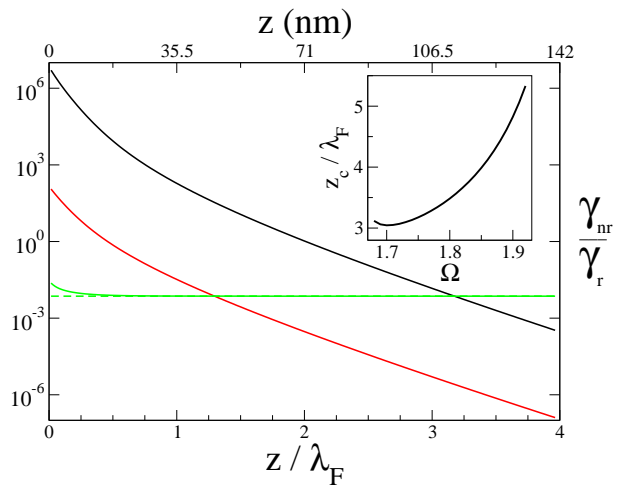


FIG. 2. Distance dependence for the decay channels γ_i for doped graphene for $\Omega = 1.75$. Black solid line: γ_1 . Red solid line: γ_2 . Green solid line: γ_3 . Green dashed line: γ_t . Inset: crossover length as a function of frequency. (Numerical values correspond to $\lambda = 500\text{nm}$ and electronic density $n = 10^{12}\text{cm}^{-2}$)

In Fig. 2, the distance dependence of the various decay channels is shown for $\Omega = 1.75$ as obtained numerically. The response is controlled by the singular features in the dispersion relation, leading to an exponential distance law. The transverse decay channel γ_3 is almost entirely due to the transverse plasmon mode γ_t , and dominates the long-distance behavior beyond a crossover length, z_c , whose frequency dependence is shown in the inset of Fig. 2. We finally note, that the extremely slow decay rate of γ_t as well as the large distance required for the onset of the power law in Eq. (15c) can be linked to the condition $1 - d_t \chi_t \approx 0$.

IV. SUMMARY

We first studied the fluorescence quenching efficacy of undoped graphene as function of distance, including transverse decay channels, retardation and graphene-field coupling to all orders. For shorter distances, we confirm the validity of previous lowest-order, unretarded results, albeit with modifications in range and saturation value. Retardation changes the distance law to $(\lambda/z)^2$, with both longitudinal (charged) and transverse (chargeless) graphene's excitation contributing to it, the latter dominating in the truly large distance asymptotic regime.

A compact, virtually exact analytical expression has been obtained for the zero-doping fluorescence yield for all distances. It involves only α and z/λ , and, therefore, endows graphene's fluorescence quenching measurements with the unique status of a fundamental ruler.

We also showed that measurements of the fluorescence quenching efficacy of doped graphene at appropriate frequencies and large distances give direct evidence of the

existence of transverse plasmons unique to two-band materials like graphene.

Finally, we note that our results might also be important because non-radiative decay of fluorescent materials amounts to electron-hole (carrier) generation in graphene. Direct (propagating field) photo-generation of carriers is inefficient in graphene (absorption $\approx \pi\alpha$), whereas indirect photo-generation by the evanescent field (that is, fluorescence quenching) can be very effective, ultimately controlled by the dye's absorption and quantum yield. This suggests new ways of enhancing graphene's photo-responsivity³¹⁻³³.

V. ACKNOWLEDGMENTS

This work has been supported by FCT under grant PTDC/FIS/101434/2008 and MIC under grant FIS2010-21883-C02-02.

Appendix A: Explicit form of decay rates

Here we outline the derivation of the non-radiative decay channels at zero doping

$$\hbar\gamma_{nr} = -2\omega^2 p_\alpha^* \left\{ \frac{1}{(2\pi)^2} \int_{q>\omega/c} d^2q \operatorname{Im} \mathcal{D}^{\alpha\beta}(z, z) \right\} p_\beta. \quad (\text{A1})$$

As the non-radiative decay rate only exists in the presence of graphene, we classify its contributions according to the nature of graphene's excitations: longitudinal (charged) and transverse. Longitudinal (l) excitations couple to both in-plane ($p_{||}$) and out-of-plane (p_z) components of the dipole matrix elements. Graphene's transverse (t) excitations only couple to the in-plane ($p_{||}$) dipole matrix element. Therefore, we write for the non-radiative decay channels

$$\gamma_{nr} = \gamma_{l,||} + \gamma_{l,z} + \gamma_{t,||}. \quad (\text{A2})$$

Let us consider $\gamma_{l,||}$ first. Selecting the longitudinal part of Eq. (9) in Eq. (8), it is straightforward to show that Eq. (A1) leads to

$$\hbar\gamma_{l,||} = -2\omega^2 \frac{p_{||}^2}{4\pi} \int_0^\infty q' dq' e^{-2q'z} \operatorname{Im} \frac{d_l^2 \chi_l}{1 - d_l \chi_l}, \quad (\text{A3})$$

where we have traded q for q' in the integration. Notice that, although the exact (i.e. retarded) photon propagators are used, the only manifestation of light's velocity c in $\gamma_{l,||}$ would be the substitution: $v^{-2} \rightarrow \tilde{v}^{-2} = v^{-2} - c^{-2}$, within the square root of χ_l at zero doping. The quantitative irrelevance of this replacement makes the instantaneous approximation for $\gamma_{l,||}$ correct. The integration in Eq. (A3) then leads to the first term of γ_{nr}/γ_r given in the main text, with the dimensionless factor f_1 given by

$$\tilde{f}_1 = \frac{1}{3!x_0^4} \int_0^1 dx \frac{x^3 e^{-x/x_0} \sqrt{1-x^2}}{1-x^2 + \frac{\pi^2 \alpha_g^2}{4} x^2}, \quad (\text{A4})$$

where $x_0 = \frac{1}{4\pi} \frac{\tilde{v}}{c} \frac{\lambda}{z}$, with *graphene's fine structure constant* $\alpha_g = \frac{c}{v} \alpha$. The approximation $\tilde{f}_1 \approx 1$ holds when $x_0 \ll 1$ and $x_0^2 \left(\frac{\pi^2 \alpha_g^2}{4} - 1 \right) \ll 1$. For graphene parameters, the latter condition dominates and can be recast as $x_0 \lesssim \frac{2}{\pi \alpha_g}$ or, equivalently, $\frac{z}{\lambda} \gtrsim \frac{\alpha}{8} \approx 10^{-3}$, justifying our approximation $\tilde{f}_1 \approx 1$.

Now, we consider the non-radiative decay channel coupling graphene's longitudinal response with an out-of-plane dipole. Using Eqs. (6) and (8), Eq. (A1) leads to

$$\hbar\gamma_{l,z} = -2\omega^2 \frac{p_z^2}{2\pi} \int q' dq' e^{-2q'z} \left(1 + \frac{\omega^2}{c^2 q'^2} \right) \operatorname{Im} \frac{d_l^2 \chi_l}{1 - d_l \chi_l}. \quad (\text{A5})$$

The integration can be rewritten as the two first terms of γ_{nr}/γ_r given in the main text, where the new dimensionless factor \tilde{f}_2 , corresponding to the second term in the sum of Eq. (A5), appears. It is given by

$$\tilde{f}_2 = \frac{1}{x_0^2} \int_0^1 dx \frac{x e^{-x/x_0} \sqrt{1-x^2}}{1-x^2 + \frac{\pi^2 \alpha_g^2}{4} x^2}. \quad (\text{A6})$$

The approximation $\tilde{f}_2 \approx 1$ has the same range of validity as that of \tilde{f}_1 .

Finally, we consider graphene's transverse excitation channels. Using the transverse components of Eqs. (4) and (9) in (8), Eq. (A1) leads to

$$\hbar\gamma_{t,||} = -2\omega^2 \frac{p_{||}^2}{4\pi} \int q' dq' e^{-2q'z} \operatorname{Im} \frac{d_t^2 \chi_t}{1 - d_t \chi_t}, \quad (\text{A7})$$

an integration that can be rewritten as third term of γ_{nr}/γ_r given in the main text, with the corresponding dimensionless parameter \tilde{f}_3 given by

$$\tilde{f}_3 = \frac{1}{g(2\pi^2 \alpha \frac{z}{\lambda})} \int_0^1 dx \frac{x e^{-x/x_0} \sqrt{1-x^2}}{x^2 + \left(\frac{\pi v}{2c} \alpha \right)^2 (1-x^2)}, \quad (\text{A8})$$

with the function $g(a)$ defined³⁴ as

$$g(a) = \int_0^\infty dx \frac{x e^{-x}}{x^2 + a^2} = -\operatorname{ci}(a) \cos(a) - \operatorname{si}(a) \sin(a). \quad (\text{A9})$$

The approximation $\tilde{f}_3 \approx 1$ applies for $x_0 \ll 1$, implying $\frac{z}{\lambda} \gtrsim \frac{v}{4\pi c} \approx 10^{-4}$, as stated in the main text.

The function $g(a)$ exhibits the following asymptotics³⁵:

$$\begin{aligned} g(a \gg 1) &= \frac{1}{a^2} \left(1 - \frac{3!}{a^2} + \frac{5!}{a^4} - \dots \right) \\ g(a \ll 1) &= -\log(e^C a), \end{aligned} \quad (\text{A10})$$

with Euler constant \mathcal{C} . The first limit in Eq. (A10) for $a = 2\pi^2 \alpha \frac{z}{\lambda} \gg 1$ explains the large distance asymptotic behavior of $\tilde{\gamma}_3$ as discussed in the main text.

-
- ¹ F. Bonaccorso, Z. Sun, T. Hasan, and A. C. Ferrari, *Nat. Photonics* **4**, 611 (2010).
- ² R. R. Nair, P. Blake, A. N. Grigorenko, K. S. Novoselov, T. J. Booth, T. Stauber, N. M. R. Peres, and A. K. Geim, *Science* **320**, 1308 (2008).
- ³ K. F. Mak, M. Y. Sfeir, Y. Wu, C. H. Lui, J. A. Misewich, and T. F. Heinz, *Phys. Rev. Lett.* **101**, 196405 (2008).
- ⁴ P. Blake, E. W. Hill, A. H. C. Neto, K. S. Novoselov, D. Jiang, R. Yang, T. J. Booth, and A. K. Geim, *Appl. Phys. Lett.* **91**, 063124 (2007).
- ⁵ A. Vakil and N. Engheta, *Science* **332**, 1291 (2011).
- ⁶ F. Xia, T. Mueller, Y.-m. Lin, A. Valdes-Garcia, and P. Avouris, *Nat. Nanotech.* **4**, 839 (2009).
- ⁷ P. Avouris, *Nano Lett.* **10**, 4285 (2010).
- ⁸ M. Jablan, H. Buljan, and M. Soljačić, *Phys. Rev. B* **80**, 245435 (2009).
- ⁹ F. H. L. Koppens, D. E. Chang, and F. J. García de Abajo, *Nano Lett.* **11**, 3370 (2011).
- ¹⁰ A. Y. Nikitin, F. Guinea, F. J. Garcia-Vidal, and L. Martin-Moreno, arXiv:1104.3558 (2011).
- ¹¹ E. Treossi, M. Melucci, A. Liscio, M. Gazzano, P. Samori, and V. Palermo, *J. Am. Chem. Soc.* **131**, 15576 (2009).
- ¹² J. Kim, L. J. Cote, F. Kim, and J. Huang, *J. Am. Chem. Soc.* **132**, 260 (2010).
- ¹³ Z. Chen, S. Berciaud, C. Nuckolls, T. F. Heinz, and L. E. Brus, *ACS Nano* **4**, 2964 (2010).
- ¹⁴ K. P. Loh, Q. Bao, G. Eda, and M. Chhowalla, *Nat. Chem.* **2**, 1015 (2010).
- ¹⁵ L. Qu, R. Martin, W. Huang, K. Fu, D. Zweifel, Y. Lin, Y. Sun, C. Bunker, B. Harruff, J. Gord, et al., *J. Chem. Phys.* **117**, 8089 (2002).
- ¹⁶ N. Nakayama-Ratchford, S. Bangsaruntip, X. Sun, K. Welsher, and H. Dai, *J. Am. Chem. Soc.* **129**, 2448 (2007).
- ¹⁷ A. Sagar, K. Kern, and K. Balasubramanian, *Nanotechnology* **21**, 015303 (2010).
- ¹⁸ K. A. Velizhanin and A. Efimov, ArXiv:1104.0233 (2011).
- ¹⁹ S. A. Mikhailov and K. Ziegler, *Phys. Rev. Lett.* **99**, 016803 (2007).
- ²⁰ T. Förster, *Ann. Phys.* **437**, 55 (1948).
- ²¹ R. R. Chance, A. Prock, and R. Silbey, *Adv. Chem. Phys.* (1978).
- ²² Y. Lin, K. Zhang, W. Chen, Y. Liu, Z. Geng, J. Zeng, N. Pan, L. Yan, X. Wang, and J. G. Hou, *ACS Nano* **4**, 3033 (2010).
- ²³ A. V. Klekachev, M. Cantoro, M. H. van der Veen, A. L. Stesmans, M. M. Heyns, and S. De Gendt, *Physica E* **43**, 1046 (2011).
- ²⁴ B. N. J. Persson and N. D. Lang, *Phys. Rev. B* **26**, 5409 (1982).
- ²⁵ C. S. Yun, A. Javier, T. Jennings, M. Fisher, S. Hira, S. Peterson, B. Hopkins, N. O. Reich, and G. F. Strouse, *J. Am. Chem. Soc.* **127**, 3115 (2005).
- ²⁶ R. S. Swathi and K. L. Sebastian, *J. Chem. Phys.* **130**, 086101 (2009).
- ²⁷ L. Novotny and B. Hecht, *Principles of Nano-Optics* (Cambridge University Press, Cambridge, England, 2006).
- ²⁸ K. W. K. Shung, *Phys. Rev. B* **34**, 979 (1986).
- ²⁹ A. Principi, M. Polini, and G. Vignale, *Phys. Rev. B* **80**, 075418 (2009).
- ³⁰ T. Stauber and G. Gómez-Santos, *Phys. Rev. B* **82**, 155412 (2010).
- ³¹ M. Begliarbekov, O. Sul, J. Santanello, X. Ai, Nan a nd Zhang, E.-H. Yang, and S. Strauf, *Nano Letters* **11**, 1254 (2011), <http://pubs.acs.org/doi/pdf/10.1021/nl1042648>, URL <http://pubs.acs.org/doi/abs/10.1021/nl1042648>.
- ³² S. Thongrattanasiri, F. H. L. Koppens, and F. J. García de Abajo, arXiv:1106.4460 (2011).
- ³³ T. Echtermeyer, L. Britnell, P. Jasnós, A. Lombardo, R. Gorbachev, A. Grigorenko, A. Geim, A. Ferrari, and K. Novoselov, ArXiv:1107.4176 (2011).
- ³⁴ I. S. Gradshteyn and I. M. Ryzhik, *Table of Integrals, Series, and Products* (Academic Press, Orlando, Florida, 1980).
- ³⁵ *Digital Library of Mathematical Functions* (2011), URL <http://dlmf.nist.gov/6>.